Check for updates

An efficient iodide ion chemosensor and a rewritable dual-channel security display material based on an ion responsive supramolecular gel†

Qi Lin, [iD] *[a] Lu Liu,[a] Juan Liu,*[b] Feng Zheng,[a] You-Ming Zhang, [iD] [a] Hong Yao[a] and Tai-Bao Wei [iD] *[a]

By introducing multi-self-assembly driving forces, coordination binding sites and signal groups into the same molecule, a well designed functional gelator **G1** was synthesized. The gelator **G1** could form a stable Pb^{2+}-coordinated supramolecular metallogel (**PbG**) accompanied with aggregation-induced fluorescence emission (AIE). **PbG** shows the reversible selective fluorescent response for I$^-$ under a gel–gel state. The detection limit of **PbG** for I$^-$ is 1.0×10^{-7} M. The AIE fluorescence of **PbG** could be reversibly switched "on–off–on" under gel–gel states *via* alternatively adding I$^-$ and Pb^{2+} water solution into **PbG**. Other anions could not induce similar stimuli-response for **PbG**. Interestingly, when a writing brush dipped in I$^-$ water solution was used to write on the xerogel film of **PbG**, the film did not show any color changes. However under UV at 365 nm, a clear dark writing image appeared. This dark writing could be erased by brushing Pb^{2+} on the film. More interestingly, when the **PbG** film containing the invisible I$^-$ writing was exposed to iodine vapor, a clear brown writing appeared on the film. However, when this film was placed under the room atmosphere for one minute, the brown writing gradually disappeared. Therefore, the **PbG** film could act as not only a convenient reversible I$^-$ detection test kit, but also an erasable dual-channel security display material.

1. Introduction

In recent years, stimuli-responsive gels,[1–8] as a type of smart supramolecular materials, have become one of the most significant realms due to their wide application prospects in chemosensors,[9–12] biomaterials,[13–16] displays,[17] physical materials,[18–22] chemical engineering[23–26] and other relevant areas.[27–32] Taking advantage of the dynamic and reversible nature of noncovalent interactions, such as strong van der Waal's forces, hydrogen bonds and π–π stacking,[33] the stimuli-responsive supramolecular gels can sense, process and actuate a response to an external change without assistance.[34–36] Moreover, metal ions-coordinated supramolecular gels[37] have become a focus due to their tunable coordination binding strength and fascinating redox, optical, electronic, as well as magnetic properties of the metal ions.[38,39] These excellent properties would bring benefit to the applications of smart materials.

However, although a significant amount of effort has been devoted to the development of metal ions coordinated supramolecular gels,[40] it is still a big challenge to design and synthesize supramolecular gels that can optically sense a given chemical stimulus with a specific selectivity. In view of this, as a part of our research interest in supramolecular chemistry,[41–45] we attempted to control the stimuli-response properties of supramolecular gels through the competitive coordination between supramolecular gelators, metal ions and guest compounds.

Herein, we designed and synthesized a gelator **G1** based on multi-assembly driving forces,[46–49] fluorescent signal groups[50] and coordination binding sites.[51,52] The gelator **G1** could form a stable supramolecular organogel in various solvents at very low critical gelation concentrations (CGCs). After the addition of Pb^{2+} to the **G1** ethanol organogel (**OG**), **OG** could form a stable Pb^{2+}-coordinated supramolecular metallogel **PbG** accompanied by the pale blue aggregation-induced fluorescence emission (AIE).[53–56] The AIE of **PbG** could be reversibly controlled by iodide anions with a specific selectivity in gel–gel states. **PbG** could act as not only a convenient reversible I$^-$ detection test kit, but also an erasable dual-channel security display material. It is worth mentioning that the security display materials have become of increasing importance.[57,58]

[a]Key Laboratory of Eco-Environment-Related Polymer Materials, Ministry of Education of China, Key Laboratory of Polymer Materials of Gansu Province, College of Chemistry and Chemical Engineering, Northwest Normal University, Lanzhou, Gansu, 730070, P. R. China. E-mail: linqi2004@126.com; weitaibao@126.com

[b]College of Chemical Engineering, Northwest University for Nationalities, Lanzhou, 730000, P. R. China. E-mail: liujuan656@126.com

† Electronic supplementary information (ESI) available. See DOI: 10.1039/c7ra06238a

2. Experimental

As show in Scheme 1, the compound 3,4,5-tris(hexadecyloxy)benzohydrazide was synthesized according to the literature-reported methods.[59] **G1** was synthesized as follow: *p*-nitrobenzaldehyde (1 mmol), 3,4,5-tris(hexadecyloxy)-benzohydrazide (1 mmol) and acetic acid (0.1 mL, as a catalyst) were added to ethanol (20 mL). Then, the reaction mixture was stirred under refluxed conditions for 24 hours. After the solvent was removed, the precipitated **G1** was yielded and recrystallized with $CHCl_3$–EtOH to get the solid **G1**. Yield: 60%, m.p.: 106–110 °C, ^{1}H NMR (400 MHz, $CDCl_3$, Fig. S1†) δ 9.30 (s, –NH, 1H), 8.26 (d, $J = 8.7$ Hz, –ArH, –CH, 3H), 7.90 (s, –ArH, 2H), 7.07 (s, ArH, 2H), 4.01 (d, $J = 3.8$ Hz, –CH_2, 6H), 1.95–1.71 (m, –CH_2, 6H), 1.36 (m, –CH_2, 78H), 0.88 (t, $J = 6.5$ Hz, –CH_3, 9H). ^{13}C NMR (150 MHz, $CDCl_3$, Fig. S2†) δ 152.76, 123.99, 107.96, 77.19, 76.98, 76.77, 73.59, 73.46, 69.44, 69.16, 60.93, 31.91, 30.30, 29.70, 29.64, 29.62, 29.55, 29.40, 29.38, 29.35, 29.30, 26.06, 22.67, 14.38, 14.08; IR (KBr, cm^{-1}) v: 3455 (–NH), 1715 (C=O), 1650 (CH=N). Anal. calcd. for $C_{62}H_{107}N_3O_6$: C 75.03, H 10.40, N 3.98; found: C 75.12, H 10.56, N 3.85. MS: ESI $[M + H]^+$ *m/z* (Fig. S3†) found: 990.8284, calcd: 990.8233.

3. Results and discussion

First, we carefully investigated the gelation properties of **G1**. As shown in Table S1,† the gelator **G1** could form a stable supramolecular organogel in various solvents at very low critical gelation concentrations. Among these solvents, the gelator **G1** showed the lowest CGC (0.40%, wt/v%, 10 mg mL^{-1} = 1%) and the highest gel–sol transition temperature (78 °C) in ethanol. The **G1**-based supramolecular organogel **OG** in ethanol is more stable than the gel in other solutions. Therefore, we investigated the influence of metal ions on the **G1** organogel in ethanol.

Interestingly, after the addition of Pb^{2+} to the **G1** ethanol organogel (**OG**), **OG** could form a stable Pb^{2+}-coordinated supramolecular metallogel **PbG**. As shown in Fig. 1, **PbG** has no fluorescence emission in hot ethanol solution ($T > T_{gel}$). However, when the temperature of this hot ethanol solution dropped below the T_{gel} of **PbG**, the emission intensity at 340 nm showed an evident increase and reached a steady state, which indicated that the fluorescence emission of metallogel **PbG** was aggregation-induced emission (AIE).

The anion response capability of the supramolecular metallogel **PbG** was primarily investigated by adding various anions in water solutions (AcO⁻, HSO_4^-, $H_2PO_4^-$, F⁻, Cl⁻, Br⁻, I⁻, N_3^-,
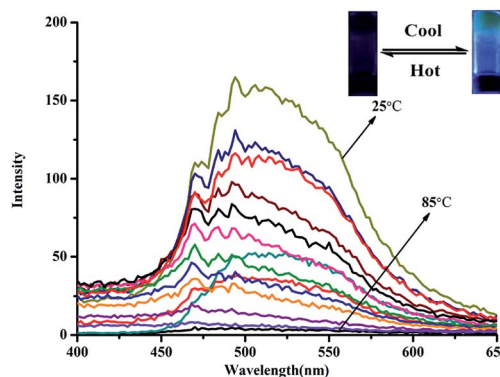

Fig. 1 Temperature dependent fluorescent spectra of the **PbG** (1%, in ethanol, **G1**–Pb^{2+} = 1 : 1) during gelation process (λ_{ex} = 340 nm). The temperature was decreased from 85 °C to 25 °C and a fluorescence spectrum was recorded every 5 °C.

SCN⁻, ClO_4^-, CN⁻, CO_3^{2-}, S^{2-} and SO_4^{2-}, 1 mol L^{-1}) to **PbG**. As shown in Fig. 2, when adding water solutions of various anions to the small amount of metallogel **PbG** on a spot plate, only I⁻ could quench the fluorescence of **PbG**, while other anions could not. These results indicated that **PbG** could selectively sense I⁻, which was attributed to I⁻ competitively binding with Pb^{2+}.

Moreover, the I⁻ response properties of **PbG** were investigated by fluorescence titrations. As shown in Fig. 3, with the addition of I⁻ into **PbG**, the spectra showed evident red shifts, which was attributed to the coordination of I⁻ with Pb^{2+}. In **PbG**, Pb^{2+} coordinated with the gelator through the acylhydrazone moiety. When I⁻ was added into **PbG**, Pb^{2+} coordinated with I⁻ and the acylhydrazone moiety was released, which induced the fluorescence spectra of the gel to undergo the red shifts. In addition, the emission intensity at 474 nm decreased with increasing the concentration of I⁻. The detection limit of the fluorescence spectra changes, which was calculated on the basis of $3\delta/S$,[60] was 2.037×10^{-6} M (Fig. S4†) for I⁻ anion.

Interestingly, after the addition of Pb^{2+} into the I⁻ containing **PbG**, the fluorescence of **PbG** recovered, which was attributed to the Pb^{2+} coordination with **G1** again. These properties
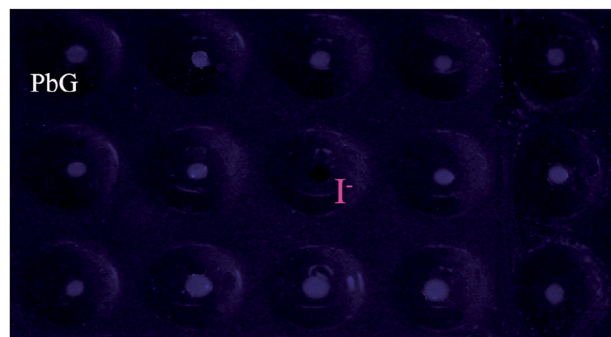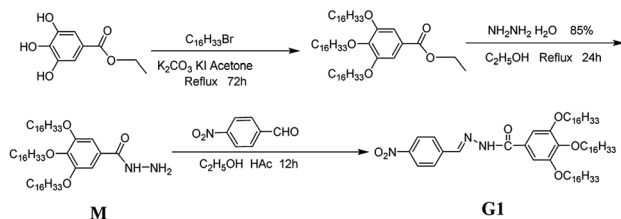

Fig. 2 Photograph of **PbG** (1%, in ethanol, **G1**–Pb^{2+} = 1 : 1) selectively detects I⁻ in the presence of various anions (5 equiv.), from left to right and top to bottom are free **PbG**, **PbG** + AcO⁻, HSO_4^-, $H_2PO_4^-$, F⁻, Cl⁻, Br⁻, I⁻, N_3^-, SCN⁻, ClO_4^-, CN⁻, CO_3^{2-}, S^{2-} and SO_4^{2-}, respectively, on a spot plate under UV at 365 nm.

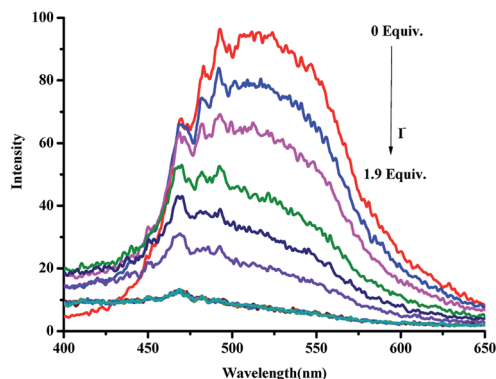**Scheme 1** The synthetic route of organogelator **G1**.

Fig. 3 Fluorescence spectra of **PbG** (1%, in ethanol, **G1**–Pb^{2+} = 1 : 1) with increasing concentration of I$^-$ (using 1 mol L^{-1} TBA in water solution as the I$^-$ sources), λ_{ex} = 340 nm.

Fig. 5 Writing, erasing and coloration of a natural light invisible image on a **PbG** supramolecular gel film (obtained from 1% ethanol metallogel, **PbG**, **G1**–Pb^{2+} = 1 : 1. Writing: write in I$^-$ water solution; erasing: brush Pb^{2+} water solution; coloration: expose the **PbG** film into the iodine vapor *ca.* 5 s). The photographs were taken at room temperature under room light and exposed to a 365 nm UV light.

make **PbG** act as an I$^-$ and Pb^{2+} controlled "on–off–on" fluorescent switch. By alternate addition of I$^-$ and Pb^{2+}, the switching could be performed reversibly at least for three cycles with a small fluorescent efficiency loss (Fig. 4).

In order to facilitate the use of the metallogel **PbG**, the I$^-$ detection film based on **PbG** was prepared by pouring the heated ethanol solution of **PbG** onto a clean glass surface and then drying in air. The **PbG** film was white under natural light and showed a blue fluorescence emission under UV at 365 nm. When a writing brush dipped in I$^-$ water solution was used to write on the film, the film did not show any color changes. However, under UV at 365 nm, a clear dark writing image appeared (Fig. 5). This dark writing image could be erased by brushing Pb^{2+} on the film. More interestingly, when the **PbG** film containing the invisible I$^-$ writing was exposed to iodine vapor, a clear brown writing appeared on the film. However, when the film was put under the room atmosphere for one minute, the brown writing disappeared gradually. Therefore, the **PbG** film could act as not only a convenient reversible I$^-$ detection test kit, but also an erasable dual-channel security display material.

In order to investigate the self-assembly and stimuli-response mechanism of **PbG**, a series of experiments was
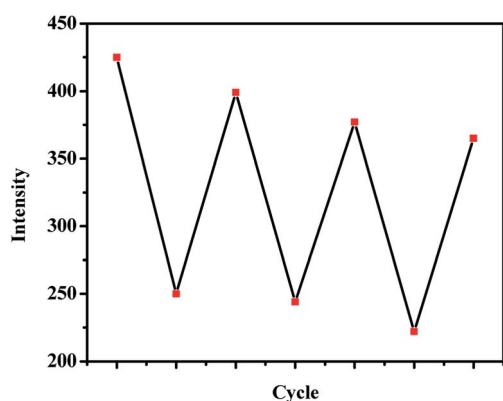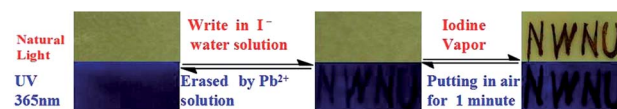
carried out. First, in the concentration dependent ^{1}H NMR of **G1** (Fig. 6), the –NH– (H_b) and –N=CH– (H_a) resonance signals showed significant downfield shifts as the concentration of **G1** rose. These results revealed that in the gelation process, the –NH– (H_b) and –N=CH– (H_a) groups formed hydrogen bonds with the –C=O groups on the adjacent gelators. On the other hand, with a gradual increase in concentration, the ^{1}H NMR signal of phenyl protons (H_c, H_d, H_e, and H_f) showed an evident upfield shift, indicating that the π–π stacking interactions between the phenyl groups involved in the gelation process.[61] Therefore, the gelator **G1** self-assembled to supramolecular organogel **OG** by the hydrogen bonds, π–π stacking as well as the vdW existing in the long alkyl chains.

The formation mechanism of supramolecular metallogel was also investigated by ^{1}H NMR titrations, as shown in Fig. 7. With the addition of Pb^{2+}, the –NH– (H_b) group on the gelator showed significant downfield shifts, which indicated that the gelator coordinated with Pb^{2+} *via* the acylhydrazone moiety. In addition, in the IR spectra (Fig. S5†) the stretching vibrations of –C=O and –C=N– of **G1** showed obviously shifts from 3455 and 1650 cm^{-1} to 3583 and 1588 cm^{-1}, respectively. These phenomena indicated that in **PbG**, Pb^{2+} coordinated with the nitrogen and oxygen atoms on the acylhydrazone group.

This presumed self-assembly and coordination mechanism was also supported by the T_{gel} of **OG** and **PbG**. For instance, as shown in Fig. 8, under the same condition, the T_{gel} of **OG** was significantly higher than that of **PbG**. The large differences of
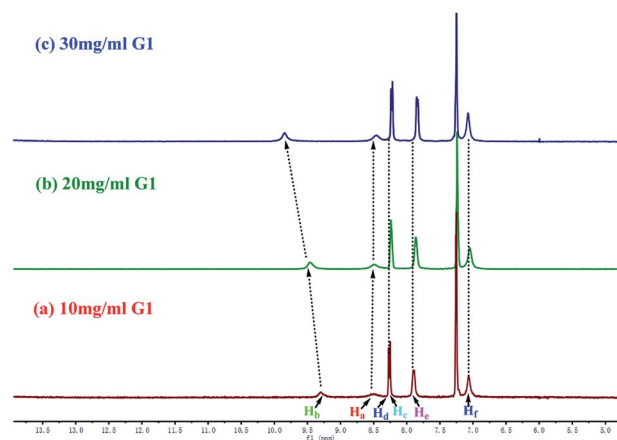

Fig. 4 Fluorescent "on–off–on" cycles of **PbG**, controlled by the alternative addition of I$^-$ and Pb^{2+}, λ_{ex} = 340 nm.

Fig. 6 Partial ^{1}H NMR spectra of **G1** in CDCl$_3$ with different concentrations.

Fig. 7 Partial ^1H NMR spectra of **G1** (2 mg mL^{-1}) and **G1** mixed with 1–7 equiv. of Pb^{2+} in ethanol-d_6.

Scheme 2 Chemical structure of the **G1** and the presumed self assembly and reversible stimuli-response mechanism.

T_{gel} between **OG** and **PbG** were ascribed to the breakage of intermolecular hydrogen bonds between –N=C–H on one gelator and –C=O on the other one in **OG**, which was caused by the coordination of Pb^{2+} with the gelator **G1**. Moreover, the Pb^{2+} coordination process reduced the distance of π–π stacking between the phenyls, which enhanced the aggregation induced emission of **PbG**.

This proposed mechanism was also supported by the XRD patterns (Fig. S6†). The XRD patterns of **OG**, **PbG** and the **PbG** treated with I$^-$ showed the peaks at $2\theta = 18.62$–$27.70°$, corresponding to the d spacing 3.5 Å, 3.45 Å, and 3.8 Å, respectively. As shown in Scheme 2 and Fig. S6,† in **OG**, the peaks at 21.28° and the d spacing 3.5 Å were attributed to the π–π stacking, which existed in the phenyl groups of **OG**. While, in **PbG**, the d spacing changed to 3.45 Å, which was attributed to the Pb^{2+} coordination process reducing the distance of π–π stacking between the phenyls. Meanwhile, the d spacing 3.8 Å was attributed to the interlamellar spacing between the supramolecular chains. In addition, after the formation of **PbG**, the peaks of **OG** (at $2\theta = 21.28, 23.22, 23.90, 25.30°$) disappeared and these peaks reappeared after **PbG** was treated with I$^-$. These phenomena confirmed that Pb^{2+} coordinated with **OG** and induced a change in the XRD pattern of **OG**, while the addition of I$^-$ into **PbG** induced the competitive coordination of I$^-$ with

Pb^{2+} and led to the recovery of XRD peaks. According to ^1H NMR, IR and XRD, the ion response mechanism of **OG** and **PbG** could be presumed as in Scheme 2.

To get further insight into the morphological features of the supramolecular organogel **OG**, metallogel **PbG** and **PbG** treated with I$^-$, SEM studies were carried out with their xerogels, respectively. As shown in Fig. S7,† the SEM images of **OG** showed an overlapped rugate layer structure. The metallogel **PbG** also showed overlapped rugate layer structures and the aggregation structure of layer was compacted. However, after I$^-$ was added into the **PbG** xerogel, the micro states experienced obvious changes. There were a large number of micro cavities formed in the xerogel of **PbG**. These micro cavities provided the **PbG** xerogel with the properties for the adsorption of iodine vapor. Therefore, the mechanism of iodine vapor-caused color change could be attributed to the iodine vapor adsorption into these micro cavities.

4. Conclusions

In summary, a novel supramolecular gelator **G1** has been designed and synthesized. The gelator **G1** could form a stable supramolecular metallogel **PbG**. Through the competitive coordination of Pb^{2+} and I$^-$ with the gelator **G1**, the aggregation-induced emission of the supramolecular metallogel **PbG** was controlled as "on–off–on". More interestingly, after Pb^{2+} competitive coordinated with I$^-$, there were a large number of micro cavities formed in the **PbG** xerogel, which enabled the **PbG** xerogel to absorb the iodine vapor and show a brown color. **PbG** could act as not only a convenient high selective and sensitive I$^-$ detection test kit, but also an erasable dual-channel secret documentation medium.
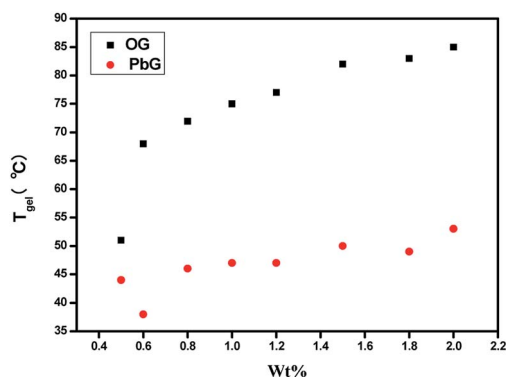
Acknowledgements

Fig. 8 Plots of T_{gel} against the concentrations of organogel **OG** and metallogels **PbG** (**G1**–Pb^{2+} = 1 : 1) in ethanol.

Notes and references

1 M. D. Segarra-Maset, V. J. Nebot, J. F. Miravet and B. Escuder, *Chem. Soc. Rev.*, 2013, **42**, 7086.

2 H. Tan, X. Ma and M. Fu, *Bull. Mater. Sci.*, 2013, **36**, 153.

3 L. Predoana, I. Stanciu, M. Anastasescu, J. M. Calderon-Moreno, M. Stoica, S. Preda, M. Gartner and M. Zaharescu, *J. Sol-Gel Sci. Technol.*, 2016, **78**, 589.

4 Z. X. Liu, Y. Feng, Z. C. Yan, Y. M. He, C. Y. Liu and Q. H. Fan, *Chem. Mater.*, 2012, **24**, 3751.

5 Q. Xia, Y. Mao, J. Wu, T. Shu and T. Yi, *J. Mater. Chem. C*, 2014, **2**, 1854.

6 S. Basak, J. Nanda and A. Banerjee, *Chem. Commun.*, 2014, **50**, 2356.

7 A. S. Lee, S. S. Choi, K. Y. Baek and S. S. Hwang, *Inorg. Chem. Commun.*, 2016, **73**, 7.

8 S. S. Babu, V. K. Praveen and A. Ajayaghosh, *Chem. Rev.*, 2014, **114**, 1973.

9 V. Lozano, R. Hernández, A. Ardá, J. Jiménez-Barbero, C. Mijangos and M. J. Pérez-Pérez, *J. Mater. Chem.*, 2011, **21**, 8862.

10 Y. He, Z. Guo, P. Jin, C. Jiao, H. Tian and W. Zhu, *Ind. Eng. Chem. Res.*, 2015, **54**, 2886.

11 C. D. Jones and J. W. Steed, *Chem. Soc. Rev.*, 2016, **45**, 6546.

12 P. Xue, J. Ding, M. Jin and R. Lu, *J. Mater. Chem. C*, 2017, **5**, 5299.

13 Q. Duan, Y. Cao, Y. Li, X. Hu, T. Xiao, C. Lin, Y. Pan and L. Wang, *J. Am. Chem. Soc.*, 2013, **135**, 10542.

14 G. Visioli, A. Comastri, D. Imperiale, G. Paredi, A. Faccini and N. Marmiroli, *Food Anal. Methods*, 2016, **9**, 469.

15 J. Jielile, A. Jialili, G. Sabirhazi, N. Shawutali, D. Redati, J. Chen, J. Bai and K. Aldyarhan, *Appl. Biochem. Biotechnol.*, 2012, **166**, 521.

16 Y. Cao, Y. Li, X. Y. Hu, X. Zou, S. Xiong, C. Lin and L. Wang, *Chem. Mater.*, 2015, **27**, 1110.

17 J. Zhou, X. Du, Y. Gao, J. Shi and B. Xu, *J. Am. Chem. Soc.*, 2014, **136**, 2970.

18 G. Sun, J. Xiao, M. Lu, H. Wang, X. Chen, Y. Yu, Y. Pan and Y. Wang, *Appl. Biochem. Biotechnol.*, 2015, **175**, 400.

19 T. Kitahara, M. Shirakawa, S. Kawano, U. Beginn, N. Fujita and S. Shinkai, *J. Am. Chem. Soc.*, 2005, **127**, 14980.

20 X. Y. Hu, T. Xiao, C. Lin, F. Huang and L. Wang, *Acc. Chem. Res.*, 2014, **47**, 2041.

21 G. Mun, H. Choi, N. Im, J. Ahn, J. Park, H. Seo, Y. Choi, J. H. Lee and J. H. Jung, *RSC Adv.*, 2017, **7**, 26827.

22 C. Kim, K. Y. Kim, J. H. Lee, J. Ahn, K. Sakurai, S. S. Lee and J. H. Jung, *ACS Appl. Mater. Interfaces*, 2017, **9**, 3799.

23 E. P. Simonenko, A. V. Derbenev, N. P. Simonenko, V. G. Sevastyanov and N. T. Kuznetsov, *Russ. J. Inorg. Chem.*, 2015, **60**, 1444.

24 Z. Cheng, J. Liao, B. He, F. Zhang, F. Zhang, X. Huang and L. Zhou, *ACS Sustainable Chem. Eng.*, 2015, **3**, 1677.

25 M. Jiang, J. Zhu, C. Chen, Y. Lu, Y. Ge and X. Zhang, *ACS Appl. Mater. Interfaces*, 2016, **8**, 3473.

26 Y. Cao, X. Y. Hu, Y. Li, X. Zou, S. Xiong, C. Lin, Y. Z. Shen and L. Wang, *J. Am. Chem. Soc.*, 2014, **136**, 10762.

27 N. V. V. Satya Bhushan and R. N. Nayak, *J. Oral Maxillofac. Surg.*, 2010, **9**, 119.

28 J. A. Foster, K. K. Damodaran, A. Maurin, G. M. Day, H. P. G. Thompson, G. J. Cameron, J. C. Bernal and J. W. Steed, *Chem. Sci.*, 2017, **8**, 78.

29 H. Wang, X. Ji, Z. Li, C. N. Zhu, X. Yang, T. Li, Z. L. Wu and F. Huang, *Materials Chemistry Frontiers*, 2017, **1**, 167.

30 P. Hallegot, G. Hussler, V. Jeanne-Rose, F. Leroy, F. Pineau and H. Samain, *J. Sol-Gel Sci. Technol.*, 2016, **79**, 365.

31 S. Lee and S. T. Nguyen, *Macromolecules*, 2013, **46**, 9169.

32 P. Xue, Q. Xu, P. Gong, C. Qian, A. Ren, Y. Zhang and R. Lu, *Chem. Commun.*, 2013, **49**, 5838.

33 T. Ghane, D. Nozaki, A. Dianat, A. Vladyka, R. Gutierrez, J. P. Chinta, S. Yitzchaik, M. Calame and G. Cuniberti, *J. Phys. Chem. C*, 2015, **119**, 6344.

34 N. Song, D. X. Chen, Y. C. Qiu, X. Y. Yang, B. Xu, W. Tian and Y. W. Yang, *Chem. Commun.*, 2014, **50**, 8231.

35 X. Yan, D. Xu, X. Chi, J. Chen, S. Dong, X. Ding, Y. Yu and F. Huang, *Adv. Mater.*, 2012, **24**, 362.

36 Y. M. Zhang, B. B. Shi, H. Li, W. J. Qu, G. Y. Gao, Q. Lin, H. Yao and T. B. Wei, *Polym. Chem.*, 2014, **5**, 4722.

37 Q. Lin, B. Sun, Q. P. Yang, Y. P. Fu, X. Zhu, T. B. Wei and Y. M. Zhang, *Chem.–Eur. J.*, 2014, **20**, 11457.

38 K. Lalitha, V. Sridharan, C. U. Maheswari, P. K. Vemula and S. Nagarajan, *Chem. Commun.*, 2017, **53**, 1538.

39 Y. Zhang, B. Zhang, Y. Kuang, Y. Gao, J. Shi, X. X. Zhang and B. Xu, *J. Am. Chem. Soc.*, 2013, **135**, 5008.

40 S. S. Abolmaali, A. Tamaddon, H. Najafi and R. Dinarvand, *J. Inorg. Organomet. Polym.*, 2014, **4**, 977.

41 Q. Lin, T. T. Lu, X. Zhu, B. Sun, Q. P. Yang, T. B. Wei and Y. M. Zhang, *Chem. Commun.*, 2015, **51**, 1635.

42 Q. Lin, T. T. Lu, J. C. Lou, G. Y. Wu, T. B. Wei and Y. M. Zhang, *Chem. Commun.*, 2015, **51**, 12224.

43 Q. Lin, Q. P. Yang, B. Sun, J. C. Lou, T. B. Wei and Y. M. Zhang, *RSC Adv.*, 2015, **5**, 11786.

44 Q. Lin, F. Zheng, L. Liu, P. P. Mao, Y. M. Zhang, H. Yao and T. B. Wei, *RSC Adv.*, 2016, **6**, 11928.

45 Q. Lin, P. P. Mao, L. Liu, J. Liu, Y. M. Zhang, H. Yao and T. B. Wei, *RSC Adv.*, 2017, **7**, 11206.

46 M. H. Liu and Y. Fang, *Chin. Sci. Bull.*, 2012, **57**, 4245.

47 C. Zhao, X. Zhang, K. Li, S. Zhu, Z. Guo, L. Zhang, F. Wang, Q. Fei, S. Luo, P. Shi, H. Tian and W. H. Zhu, *J. Am. Chem. Soc.*, 2015, **137**, 8490.

48 Q. Lin, Q. P. Yang, B. Sun, Y. P. Fu, X. Zhu, T. B. Wei and Y. M. Zhang, *Soft Matter*, 2014, **10**, 8427.

49 Y. Gong, T. Jiao, Q. Hu, N. Cheng, W. Xu, Y. Bi and L. Yu, *J. Phys. Chem. C*, 2015, **119**, 16349.

50 X. Ji, Y. Yao, J. Li, X. Yan and F. Huang, *J. Am. Chem. Soc.*, 2013, **135**, 74.

51 Q. Lin, B. Sun, Q. P. Yang, Y. P. Fu, X. Zhu, Y. M. Zhang and T. B. Wei, *Chem. Commun.*, 2014, **50**, 10669.

52 D. H. Qu, Q. C. Wang, Q. W. Zhang, X. Ma and H. Tian, *Chem. Rev.*, 2015, **115**, 7543.

53 Y. Hong, J. W. Y. Lam and B. Z. Tang, *Chem. Soc. Rev.*, 2011, **40**, 5361.

54 W. Lei, Y. Liu, J. Bai, Y. Dai, Y. Kan, T. Chen and B. Yin, *Tetrahedron*, 2015, **71**, 5465.

55 K. Duraimurugan, J. Sivamani, M. Sathiyaraj, V. Thiagarajan and V. Siva, *J. Fluoresc.*, 2016, **26**, 1211.

56 X. Wu, H. Li, Y. Kan and B. Yin, *Dalton Trans.*, 2013, **42**, 16302.

57 A. Kishimura, T. Yamashita, K. Yamaguchi and T. Aida, *Nat. Mater.*, 2005, **4**, 546.

58 N. Tamaoki, A. V. Parfenov, A. Masaki and H. Matsuda, *Adv. Mater.*, 1997, **9**, 1102.

59 Y. P. Fu, Q. Lin, T. B. Wei, P. Chen, X. Zhu, X. Liu and Y. M. Zhang, *Chem. Reagents*, 2013, **35**, 367.

60 Analytical Methods Committee, *Analyst*, 1987, **112**, 199.

61 C. Po, Z. Ke, A. Y. Y. Tam, H. F. Chow and V. W. W. Yam, *Chem.–Eur. J.*, 2013, **19**, 15735.